

Injectable Biocompatible and Biodegradable pH-Responsive Hollow Particle Gels Containing Poly(acrylic acid): The Effect of Copolymer Composition on Gel Properties

Silvia S. Halacheva,^{*,†} Daman J. Adlam,[‡] Eseelle K. Hendow,[§] Tony J. Freemont,^{‡,||} Judith Hoyland,^{‡,||} and Brian R. Saunders^{*,§}

[†]Institute for Materials Research and Innovation, University of Bolton, Deane Road, Bolton, Greater Manchester, BL3 5AB, United Kingdom

[‡]Centre for Tissue Injury and Repair, Institute of Inflammation and Repair, Faculty of Medical and Human Sciences, University of Manchester, Oxford Road, Manchester, M13 9PT, United Kingdom

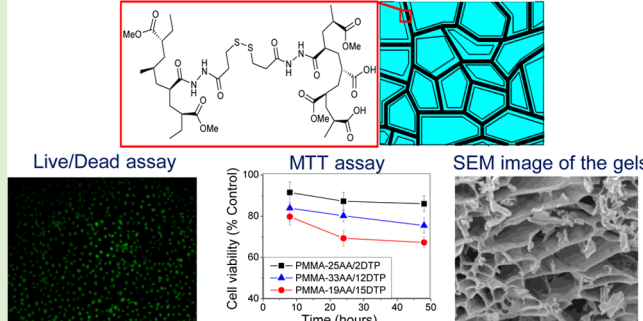
^{||}NIHR Manchester Musculoskeletal Biomedical Research Unit, Manchester Academic Health Science Centre, Manchester, M13 9NT, United Kingdom

[§]School of Materials, University of Manchester, Grosvenor Street, Manchester, M13 9PL, United Kingdom

Supporting Information

ABSTRACT: The potential of various pH-responsive alkyl (meth)acrylate ester- and (meth)acrylic acid-based copolymers, including poly(methyl methacrylate-*co*-acrylic acid) (PMMA-AA) and poly(*n*-butyl acrylate-*co*-methacrylic acid) (PBA-MAA), to form pH-sensitive biocompatible and biodegradable hollow particle gel scaffolds for use in non-load-bearing soft tissue regeneration have been explored. The optimal copolymer design criteria for preparation of these materials have been established. Physical gels which are both pH- and redox-sensitive were formed only from PMMA-AA copolymers. MMA is the optimal hydrophobic monomer, whereas the use of various COOH-containing monomers, e.g., MAA and AA, will always induce a pH-triggered physical gelation. The PMMA-AA gels were prepared at physiological pH range from concentrated dispersions of swollen, hollow, polymer-based particles cross-linked with either cystamine (CYS) or 3,3'-dithiodipropionic acid dihydrazide (DTP). A linear relationship between particle swelling ratios, gel elasticity, and ductility was observed. The PMMA-AA gels with lower AA contents feature lower swelling ratios, mechanical strengths, and ductilities. Increasing the swelling ratio (e.g., through increasing AA content) decreased the intraparticle elasticity; however, intershell contact and gel elasticity were found to increase. The mechanical properties and performance of the gels were tuneable upon varying the copolymers' compositions and the structure of the cross-linker. Compared to PMMA-AA/CYS, the PMMA-AA/DTP gels were more elastic and ductile. The biodegradability and cytotoxicity of the new hollow particle gels were tested for the first time and related to their composition, mechanical properties, and morphology. The new PMMA-AA/CYS and PMMA-AA/DTP gels have shown good biocompatibility, biodegradability, strength, and interconnected porosity and therefore have good potential as a tissue repair agent.

pH- and Redox-Responsive Hollow PMMA-AA/DTP Particle Gel Scaffolds



INTRODUCTION

Hydrogel scaffolds have been used extensively in tissue engineering and cell replacement therapies because their structure and properties can be easily optimized.^{1,2} The scaffold provides a three-dimensional structure for the growth of cells while maintaining their differentiated function. A range of natural substances such as collagen I, chitosan, fibrinogen, agarose, and alginate have been investigated as cell-carrying scaffolds^{1,3–5} and synthetic polymer-based hydrogel scaffolds have also been explored.^{6–12} The principal advantage of synthetic materials is that their porosity, mechanical strength, and degradation rate can be easily tuned by varying the

structures of the polymer and/or the cross-linker and the extent of interchain cross-links in the hydrogel's matrix.^{13–16} In order to facilitate their rapid and efficient removal from the body, a range of disulfide-based cross-linkers have been investigated, as the disulfide linkage can be readily cleaved to the corresponding thiol(s) in the presence of endogenous reducing agents such as glutathione.^{11,17–20} Shu et al.²¹ prepared thiol-modified hyaluronic acid (HA) using carbodiimide-mediated hydrazide

Received: February 10, 2014

Revised: March 26, 2014

Published: March 31, 2014

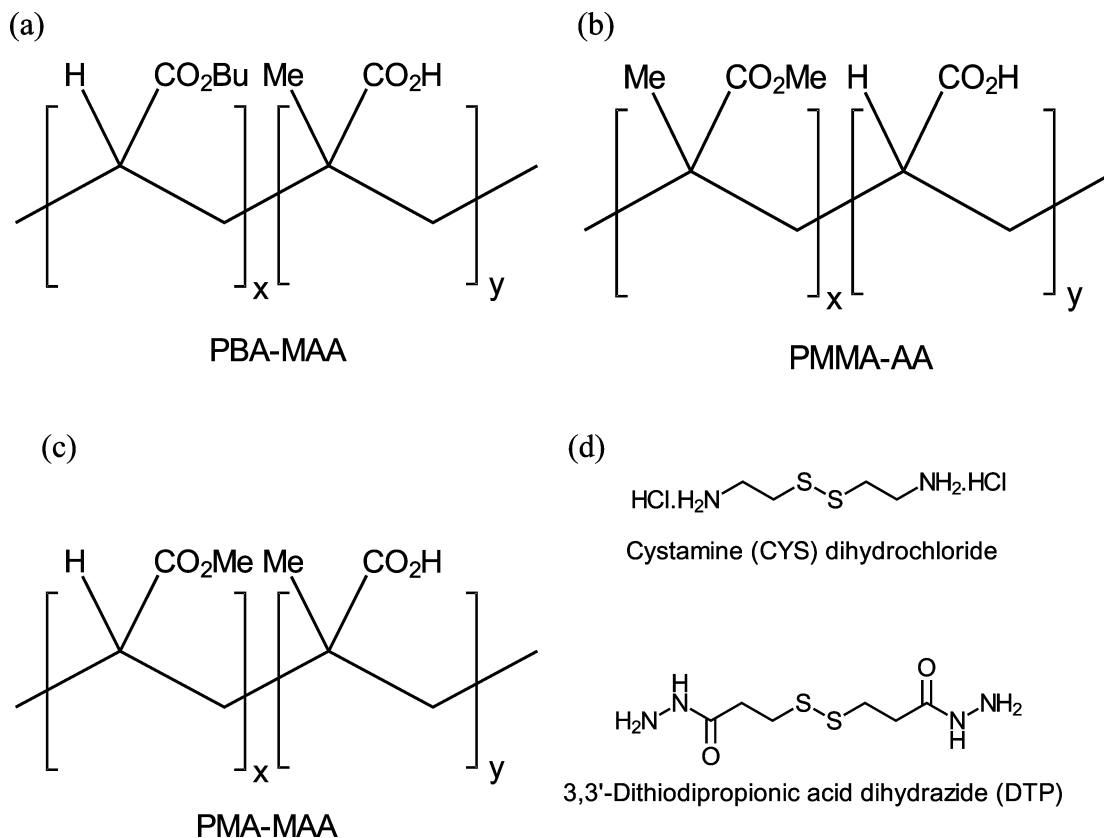


Figure 1. Copolymer and cross-linker structures.

chemistry. The HA hydrogels were then formed under physiological conditions by oxidation of the thiol groups to disulfides. Ghosh et al.²² cross-linked thiol-modified HA with poly(ethylene glycol) diacrylate (PEGDA) to form hydrogels. Lee et al.²³ developed a HA/Pluronic composite with tissue adhesive properties. Hydrogel scaffolds embedded with chondrocyte are currently one of the most promising approaches for cartilage regeneration.²⁴ The hydrogels were mixed with chondrocytes and injected into the body. Injectable polymer/cell dispersions have emerged as a superior and minimally invasive alternative for tissue regeneration.^{25,26} The injectable therapy could eliminate post-treatment complications, significantly improve patient comfort, and shorten recovery time. Injectable hydrogel scaffolds are also being used for nonload bearing bone and soft tissue repair. These hydrogels featured low mechanical strength and were used only as a cell delivery vehicle. Lee et al.²⁷ mixed primary rat alveolar osteoblasts with a poly(aldehyde guluronate)-based hydrogel and injected the resulting mixture into the spines of mice. In this system, mineralized bone was observed to form over a period of nine weeks. Similarly, Lisignoli et al.²⁸ seeded a HA-based gel scaffold with bone marrow stromal cells and implanted this into a rat model critical radial defect, leading to defect mineralization and subsequent healing. Kondu et al.²⁹ used a silk sericin/poly(acrylamide) hydrogel network as a reconstructive dermal sealant. Their system demonstrated rapid gelation, high porosity, cell adhesion, and compressive strength of up to 61 kPa.

Recently, Liu et al.³⁰ successfully utilized dispersions of star-shaped poly((S)-lactic acid)-based hollow particles, prepared by emulsification of the polymer in glycerol, as an injectable delivery system for hyaline cartilage regeneration in rabbits.

Bird et al.³¹ prepared hollow poly(methyl methacrylate-*co*-methacrylic acid)- (PMMA-MAA) and poly(ethyl acrylate-*co*-methacrylic acid)-based (PEA-MAA) particles that are both pH-responsive and redox-sensitive via a solvent evaporation approach. After being cross-linked with CYS, the hollow particles swelled within the physiological pH range and also formed physical gels from their concentrated dispersions. The gels had micrometer-scale interconnected porosity and were rapidly disassembled upon addition of glutathione. We have also previously explored new types of high-porosity, high-elasticity PMMA-MAA and PEA-MAA particle gels,³² which are potentially suitable for future use in minimally invasive tissue repair. A physiologically compatible strategy for preparation of the PMMA-MAA and PEA-MAA particle-based gels was employed, utilizing DTP or CYS as cross-linking agents. A key finding of the study was that for cross-linked particles of similar composition the formation of considerably more elastic and ductile gels was observed from the most lightly cross-linked particles. Furthermore, compared to the PMMA-MAA/CYS and PEA-MAA/CYS gels, those formed from DTP-cross-linked particles had higher elasticity, thicker pore walls, and improved interconnectivity. However, the hollow particles observed were hydrophobic at pH < pK_a and in a collapsed state, which could make cell encapsulation and growth in the gel matrices somewhat problematic.

Herein we extend considerably our earlier studies with the aim of identifying a system which meets all necessary requirements for soft tissue repair—i.e., high porosity, biocompatibility, biodegradability, and adequate mechanical strength—in order to be developed into a clinically successful treatment for tissue regeneration. In the present study we investigated PMMA-AA, PMA-MAA, and PBA-MAA copoly-

mers, establishing MMA (methyl methacrylate) to be the optimal ester (Figure 1). These systems have been chosen to allow a wide range of structural variation for the constituent pH-responsive copolymers. To investigate the effect of tuning hydrophobicity of the copolymer, their glass transition temperature and the pK_a of the particles on the gel morphology and mechanical properties we investigated the structurally related PBA-MAA and PMA-MAA copolymers for gel formation. We chose BA and MA as more hydrophobic and less hydrophobic ester subunits, respectively, compared with MMA and EA. To explore the effect of tuning the hydrophobicity of the carboxylic acid subunits we substituted the MAA in PMMA-MAA³² with the more hydrophilic AA which resulted in the formation of a series of pH-responsive PMMA-AA-based particles. These particles were subsequently cross-linked using CYS or DTP and formed mechanically strong, biodegradable hydrogels from their concentrated dispersions under physiological pH conditions. The resulting gels have been physically characterized by a variety of methods such as dynamic light scattering (DLS), optical microscopy, scanning electron microscopy (SEM), and rheology. The cytotoxicities of the new gels have also been tested and related to their composition and mechanical properties. The new gels show good biocompatibility, biodegradability, interconnected porosity and good elastic modulus values and are therefore anticipated to have excellent potential for future application as injectable gels for regenerative medicine.

EXPERIMENTAL SECTION

Materials and Methods. All chemical reagents and solvents were purchased from Sigma-Aldrich, unless otherwise stated, and used as received. Milli-Q water was used throughout, unless otherwise stated. Reactions requiring anhydrous conditions were performed in oven-dried glassware, with anhydrous solvents, under a positive pressure of nitrogen. 3,3'-Dithiodipropionic acid dihydrazide (DTP) was synthesized according to a literature method.³³

Measurements. Proton nuclear magnetic resonance (¹H NMR) spectra were recorded on Bruker Avance 400 and 500 MHz spectrometers. GPC analyses were performed on a Shodex R101 refractive index detector. Samples were dissolved in anhydrous, inhibitor-free THF (1 mg/mL) at room temperature. The columns contained Phenomenex Phenogel 5 μm beads with 500, 10⁴, and 10⁶ Å pore sizes. The flow rate was 1 mL/min. Potentiometric titration was conducted using a Mettler Toledo DL15 titrator. Measurements were performed on 40 mL of a 1 wt % non-cross-linked dispersion using standardized NaOH solutions. All pK_a values reported here are apparent values. Optical microscopy was conducted with an Olympus BX41 microscope and white transmitted light. Dispersions were deposited on SEM stubs by evaporation at room temperature. Thin sections of gel were rapidly frozen in liquid nitrogen and residual moisture removed by freeze-drying. Rheology measurements were performed at 25 °C using a TA AR-G2 rheometer and a 250 μm gap with a 20-mm-diameter steel plate at 25 °C. All strain-sweep measurements were conducted at a frequency of 1 Hz. All frequency-sweep measurements were conducted at a strain of 0.1%. A particle concentration of 5.0 wt % was used for these studies. DLS measurements were performed on a light scattering photometer consisting of a 50 mW He/Ne laser, operating at 633 nm, with a standard avalanche photodiode (APD) and 90° detection optics connected to a Malvern Zetasizer Nano ZS90 autocorrelator. The measurements were carried out at pH values ranging 6.0–10.0 and at a constant solution concentration of 0.1 wt %. The dispersions were treated with 1.0 M NaOH solution until the desired pH value was reached, then allowed to equilibrate for 15 min. The hydrodynamic diameter (D_h) of the particles was measured at 90° using a Malvern Zetasizer Nano ZS90. At least 10 correlation functions were analyzed

per sample, at each pH value, in order to obtain an average measurement. The volume swelling ratio, Q , of the PMMA-AA particles, functionalized with either CYS or DTP, was estimated using $Q = (D_h/D_{h(\text{collapse})})^3$, where D_h and $D_{h(\text{collapse})}$ are the hydrodynamic diameters of the particles at a given pH and in the collapsed nonswollen state, respectively.³² All $D_{h(\text{collapse})}$ values were measured at the lowest pH values tested. For the PMMA-AA particles the $D_{h(\text{collapse})}$ values do not correspond to the fully collapsed state of the particles.

Synthesis of Copolymers. The PMMA-AA, PMA-MAA, and PBA-MAA copolymers were synthesized via free radical polymerization of appropriate mixtures of MMA with AA and MAA with either MA or BA. The copolymer abbreviations used here identify the molar percentages of each component. For example, PMMA-27AA contains 27 mol % AA and 73 mol % MMA units. The following synthesis of PMMA-27AA is representative of the procedure employed for the other copolymers. An oven-dried flask, fitted with a condenser, was purged with nitrogen and charged with 2,2'-azobis(2-methylpropionitrile) (AIBN, 0.25 g) and anhydrous THF (85 mL). The magnetically stirred solution was heated at 55 °C, under a steady flow of nitrogen, for 30 min. A mixture of MMA (6.06 g, 0.7 equiv), AA (1.87 g, 0.3 equiv), and AIBN (0.025 g) was dissolved in anhydrous THF (17 mL) and added to the solution at a uniform rate over 90 min. After the feed the reaction mixture was heated/stirred at 70 °C for a further 18 h and then cooled to room temperature. The reaction mixture was concentrated under reduced pressure to a volume of approximately 100 mL and then poured into 1000 mL of cold water. The precipitated polymer was removed by filtration, rinsed thoroughly with water, and air-dried.

Particle Preparation. The non-cross-linked PMMA-AA, PMA-MAA, and PBA-MAA particles were prepared using a solvent evaporation approach. The following procedure is representative for the preparation of PMMA-AA and PBA-MAA particles. First, 2.00 g of copolymer was dissolved in a mixed $\text{CH}_2\text{Cl}_2:\text{MeOH}$ solvent (44 mL, 84:16, v/v). In a separate vessel, a solution of poly(vinylpyrrolidone) (PVP, 1.20 g, average MW 40 000 g·mol⁻¹) in water (120 mL) was cooled to 0 °C and sheared at 10 000 rpm, using a Silverson LR4 high speed mixer. The solution of copolymer was then added, at a uniform rate of 10 mL/min, to the aqueous PVP solution. Emulsification was continued for a further 30 s after complete addition of the polymer solution and the emulsion was then allowed to stir slowly overnight in order to remove CH_2Cl_2 . The product was purified by repeated centrifugation and redispersion in water in order to remove excess PVP. The resultant suspension was then filtered through a 50 μm filter and stored at 2–4 °C. For PMA-MAA particles prepared in this manner, centrifugation of the particle dispersions resulted in the formation of large agglomerates, which were not redispersible.

Preparation of Cross-Linked Particles. The following procedure for the preparation of PMMA-25AA/2CYS is representative of the general procedure employed: 8.8 mL of the concentrated PMMA-27AA particle stock dispersion (3.9 wt %, 1 mmol COOH groups) was diluted with 0.1 M pH 6.4 phosphate buffer solution to a volume of 22.9 mL and a final concentration of 1.5 wt %. The pH of the buffer utilized depended upon the pK_a of the particles. To the resulting stirred suspension, *N*-hydroxysuccinimide (NHS) (0.140 g, 1.22 equiv.) was added followed by *N*-(3-dimethylaminopropyl)-*N'*-ethylcarbodiimide (EDC) hydrochloride (0.153 g, 0.80 equiv). Stirring was continued for a further fifteen minutes before CYS dihydrochloride (0.113 g, 0.50 equiv) was added. The reaction mixture was then stirred at room temperature for 24 h and the cross-linked particles were isolated by centrifugation, followed by three cycles of redispersion in water and centrifugation. The DTP cross-linked particles were prepared in an analogous manner by substituting DTP for CYS dihydrochloride. The cross-linked particle abbreviation used here identifies the mol % nonfunctionalized MAA or AA groups and the mol % CYS or DTP incorporated into the particles. For example, PMMA-25AA/2CYS contained 25 mol % AA and 2 mol % CYS.

Gel Cytotoxicity Studies. T/C28a2 cells, an immortalized human chondrocyte cell-line, were cultured in Dulbecco's Modified Eagle's medium (DMEM, Gibco) supplemented with 10% fetal bovine serum (FBS, Gibco) and antibiotic/antimycotic at 37 °C in a humidified 5%

CO_2 atmosphere. Cells were seeded at a density of 6×10^4 per well onto 24 well plates containing $0.4 \mu\text{m}$ cell-culture inserts (BD Biosciences) and allowed to adhere overnight before exposure to 20 mg of PMMA-AA/CYS or PMMA-AA/DTP gels. Cell viability was determined at 8, 24, and 48 h time-points by MTT assay and at 48 h by live/dead assay (Invitrogen).

RESULTS AND DISCUSSION

Synthesis and Characterization of Copolymers.

PMMA-AA, PMA-MAA, and PBA-MAA (Figure 1) were synthesized by free-radical polymerization of appropriate mixtures of their constituent monomers. The weight average molecular weight and polydispersity of the copolymers were determined by GPC (Figure S1, Supporting Information). The copolymers had molecular weights ranging from 18 630 to 48 730 $\text{g}\cdot\text{mol}^{-1}$ (Table 1). GPC analyses gave monomodal

the methylene protons of both MMA and AA groups (Figure S2, Supporting Information). The composition of the PBA-42MAA polymer was determined from the ratios of the signal intensities of the methylene protons of the butyl ester units to the methylene protons of both BA and MAA groups (see Figure S3, Supporting Information). The experimental values obtained by ^1H NMR were in good agreement with the theoretical values (Table 1).

Non-Cross-linked Particle Preparation and Characterization.

Dispersions of PMMA-27AA-, PMMA-34AA-, PMMA-45AA-, and PBA-42MAA-based non-cross-linked particles were prepared by the sequential emulsification-solvent evaporation protocol described in the Experimental Section. In order to facilitate the formation of homogeneous and colloidally stable particle dispersions, a slow addition (10 mL/min) of the copolymer solution was performed. The dispersions thus obtained were stable for at least three months after their preparation. Representative optical micrographs of PBA-42MAA and PMMA-27AA are shown in Figure 2a and b, respectively. These images suggest formation of spherical, hollow structures with thin shells. Similar objects were also seen in aqueous dispersions of the PMMA-34AA and PMMA-45AA copolymer particles. Hollow particles have been previously reported in the aqueous dispersions of structurally analogous PMMA-MAA and PEA-MAA based particles.^{31,32,34} Compared to their PMMA-MAA and PEA-MAA based counterparts, the shell thicknesses of the PMMA-AA and PBA-MAA particles are much lower (approximately $0.6\text{--}1.0 \mu\text{m}$) which suggests that these particles are both more flexible and more easily deformed. Representative SEM images of non-cross-linked PMMA-27AA and PBA-42MAA particles are shown in Figure 3a and Figure S4, Supporting Information, respectively. Both the optical and SEM images show spherical hollow objects which range in size from 1 to $5 \mu\text{m}$. Some of the particles are crumpled while others are wrinkled; there are also particles with relatively smooth surfaces.

Table 1. Characterization Data for PMMA-AA, PMA-MAA, and PBA-MAA

Composition	$M_w (\text{g}\cdot\text{mol}^{-1})^a$	PDI ^a	mol % MAA			pK_a^c
			theor. ^b	exper. ^b	exper. ^c	
PMMA-27AA	48 730	1.93	30	27	29	7.8
PMMA-34AA	37 350	1.74	40	34	34	7.1
PMMA-45AA	18 630	1.64	50	45	48	6.8
PMA-40MAA	23 450	2.41	42	40	44	^d
PBA-42MAA	25 930	1.93	40	42	43	8.5

^aDetermined by GPC. ^bDetermined by ^1H NMR. ^cDetermined from the potentiometric titration data. ^dThe pK_a of PMA-40MAA was not determined as the copolymer did not redisperse after centrifugation.

distributions with polydispersities ranging from 1.64 to 2.41. The copolymers' structural compositions were determined from their ^1H NMR spectra in $\text{DMSO}-d_6$ (Figures S2 and S3, Supporting Information). The compositions of the PMMA-AA samples were calculated by examining the relative ratios of signal intensities of the methoxyl protons of MMA groups and

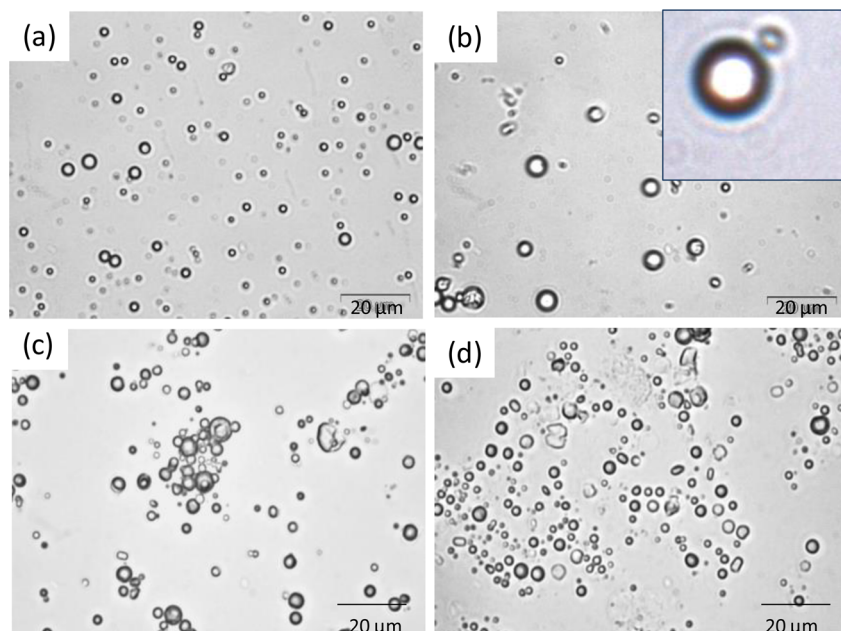


Figure 2. Optical micrographs of aqueous hollow particle dispersions: (a) PBA-42MAA ($\text{pH} = 6.5$); (b) PMMA-27AA ($\text{pH} = 7.0$); (c) PMMA-25AA/2DTP ($\text{pH} = 7.0$); (d) PMMA-42AA/3CYS ($\text{pH} = 6.5$).

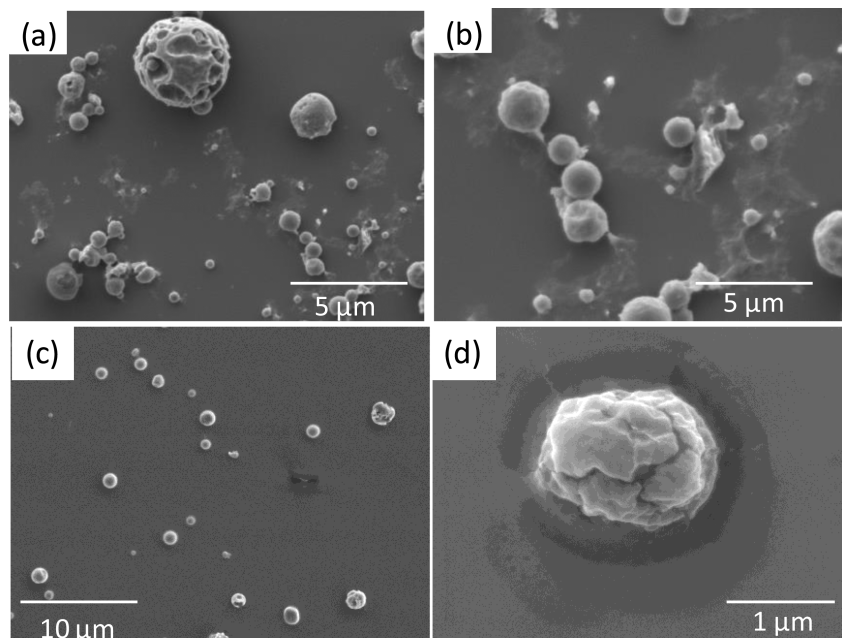


Figure 3. SEM images of aqueous hollow particle dispersions: (a) PMMA-27AA ($\text{pH} = 6.5$); (b) PMMA-25AA/2CYS ($\text{pH} = 7.0$); (c) PMMA-19AA/15DTP ($\text{pH} = 6.5$); (d) PMMA-19AA/15DTP ($\text{pH} = 6.5$).

Hollow polymer particles offer excellent potential for preparing high performance biomaterials. They have been used extensively for a large range of applications such as drug delivery,³⁵ gene delivery,³⁶ artificial cells,³⁷ and in regenerative medicine.³⁸ Polymer-based capsules have been prepared by a variety of techniques, including double emulsions, polymer precipitation by phase separation, layer-by-layer assembly, microemulsion polymerization, and vesicle formation by spontaneous self-assembly of block copolymers.^{39–43} In the aqueous dispersions of PMMA-MAA and PEA-MAA copolymer analogues, hollow particles were formed shortly after emulsification due to the polymers' precipitation at the dichloromethane droplet/water interface.^{31,32,34} The copolymers, which are insoluble in both organic solvent and aqueous phase, form shells around the dichloromethane droplets which subsequently collapse as the residual solvent evaporates.

In the present study we investigate the aqueous solution properties of five new copolymers: PMMA-27AA, PMMA-34AA, PMMA-45AA, PMA-40MAA, and PBA-42MAA. It was found that copolymers containing greater than 50 mol % (meth)acrylic acid did not form stable particle dispersions. Accordingly, these copolymers are composed mainly of either PMMA, which is relatively rigid with a higher T_g of 109 °C, or the more flexible PMA/PBA hydrophobic subunits which feature a T_g of 10 °C and –54 °C, respectively.⁴⁴ With the exception of PMA-40MAA, all of the copolymers tested formed hollow particles upon emulsification (see Figure 2). The product of PMA-40MAA emulsification did not redisperse after centrifugation which is probably due to the greater flexibility of PMA relative to the PMMA. The importance of chain rigidity in the self-assembly phenomenon has been previously documented in reports concerning aqueous solutions of PMMA-block-MAA and PMMA-block-AA.^{45,46} In contrast to these copolymers, where particles of various sizes and shapes were observed, PMA-MAA solutions showed no particle formation.

The molar percentages (mol %) of AA in the PMMA-AA and PBA-AA non-cross-linked particles were measured by potentiometric titration. The values calculated by potentiometric titration and those estimated from the ^1H NMR spectra of the copolymers were in reasonable agreement with each other and with the theoretical values (Table 1). Figure S5 (Supporting Information) shows the 'pH vs % neutralization' plots for non-cross-linked PMMA-AA and PBA-42MAA particle dispersions. The pK_a values decrease as the content of hydrophilic AA increases (see Table 1). The pK_a values for the PBA-42MAA particles were much higher than those of all corresponding PMMA-AA, PMMA-MAA, and PEA-MAA analogues,^{31,32,34} which is probably due to the higher hydrophobicity of PBA compared to PEA and PMMA.

An unexpected finding of this study was that the pK_a values of the PMMA-AA copolymers were not significantly lower than those previously reported for the structurally similar PMMA-MAA copolymers.³² The pK_a of poly(acrylic acid) is approximately one unit lower than that of poly(methacrylic acid).^{47,48} Therefore, it is reasonable to assume that the hydrophobic MMA, which is also the dominant monomer in terms of the copolymer compositions, has the major effect on the pK_a values. Substituent effects on the carboxylic acid monomer are of secondary importance for these copolymers. The finding is also consistent with the highest pK_a measured being that of PBA-42MAA. This suggests that the ionization-induced swelling transition near physiological pH would still occur when a range of different carboxylic acid-containing monomers are included in the copolymer. This type of versatility is potentially useful in the context of biomaterials.

Preparation and Characterization of Cross-Linked Particles. The earlier established EDC-mediated coupling methodology, utilizing the diamino compounds CYS and DTP as cross-linkers, was employed.^{49–51} The cross-linkers' structures are presented in Figure 1d. The compositions of the cross-linked particles were determined from elemental analyses. In all reactions, the same molar proportions of reagents (EDC, NHS, CYS/DTP) relative to the number of available COOH groups were used. For PMMA-AA, the proportion of available COOH groups which were successfully

Table 2. Cross-Linked Particle Compositions, Swelling, and Gel Properties

entry	copolymer	RCONHR ^a (%)	cross-linked copolymer particles' composition	Q _{max} ^b	pH _{G' max} ^c	G' _{max} ^d (Pa)	γ _{c(max)} ^e (%)
1	PMMA-27AA	6	PMMA-25AA/2CYS	1.4	7	300	29
2		6	PMMA-25AA/2DTP	2.9	7	400	32
3	PMMA-34AA	7	PMMA-31AA/3CYS	3.0	7	400	36
4		45	PMMA-19AA/1SDTP	2.9	7	800	38
5	PMMA-45AA	7	PMMA-42AA/3CYS	3.9	7	1500	42
6		27	PMMA-33AA/12DTP	8.3	7	5900	48
7	PBA-42MAA	3	PBA-41MAA/1DTP	-	-	-	-

^aPercentage of R¹C(O)NHR² formed. ^bSwelling ratio at pH_{G' max}. In each case this value of Q corresponded to the maximum swelling ratio. ^cpH at which gels with G'_{max} are formed. ^dThe maximum storage modulus value. ^eYield strain at pH_{G' max}. The swelling ratio, the G'_{max} and γ_{c(max)} for entry 7 was not determined, as the particles did not swell.

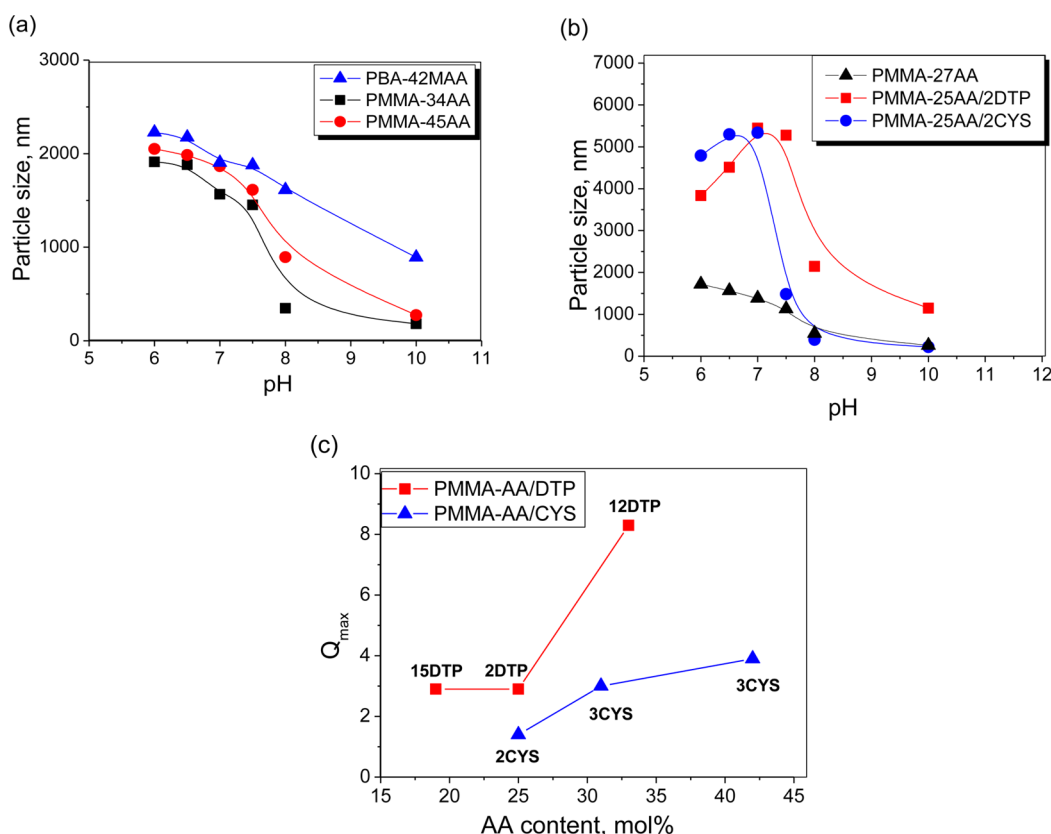


Figure 4. Variations of D_h^{slow} with the solution pH for (a) PBA-42MAA, PMMA-34AA, and PMMA-45AA non-cross-linked particles; (b) PMMA-27AA, PMMA-25AA/2DTP, and PMMA-25AA/2CYS particles; (c) variations of Q_{max} with the AA content (mol %) for PMMA-AA/DTP and PMMA-AA/CYS particles.

reacted with either CYS or DTP ranged from 6% up to 45%, whereas for the PBA-42MAA particles just 3% conversion was achieved (Table 2). All of these results were considerably lower than the theoretically predicted values which would correspond to a 100% chemical yield (see the Experimental Section). The low percentage of R¹C(O)NHR² group formation was attributed to the low level of carboxylic acid group activation at the reactions' pH values. For our studies the control of pH during the cross-linking was of critical importance, as the dispersions of non-cross-linked particles would dissolve if the solution pH reached the corresponding particles' pK_a value. Accordingly, all cross-linking reactions were performed at pH 6.4, which is well below the pK_a of the non-cross-linked particles (see Table 1). Compared to the PMMA-AA/CYS particles, the PMMA-AA/DTP particles featured higher extents of cross-linker incorporation. This finding was rationalized by the retention of nucleophilicity by the terminal nitrogen

atoms of hydrazides at acidic pH values.^{52,53} The lowest percentage of amide formation was observed for PBA-42MAA/1DTP. All attempts to cross-link the PBA-MAA particles with CYS were unsuccessful, which could be due to COOH groups being buried within the hydrophobic PBA interior and therefore not available for cross-linking at the pH employed, which was lower than the corresponding pK_a value.

Optical microscope images of the cross-linked PMMA-25AA/2DTP and PMMA-42AA/3CYS particles are presented in Figure 2c and d. For PMMA-AA/CYS or PMMA-AA/DTP particles, the spherical-hollow morphology was also apparent for the respective non-cross-linked particles (compare Figure 2b with c and d). The SEM images of PMMA-25AA/2CYS (Figure 3b) and PMMA-19AA/1SDTP (Figure 3c,d) show spherical objects. These particles show some similarities to the "golf-ball" and "polyelectrolyte capsule" morphologies reported previously.^{54,55}

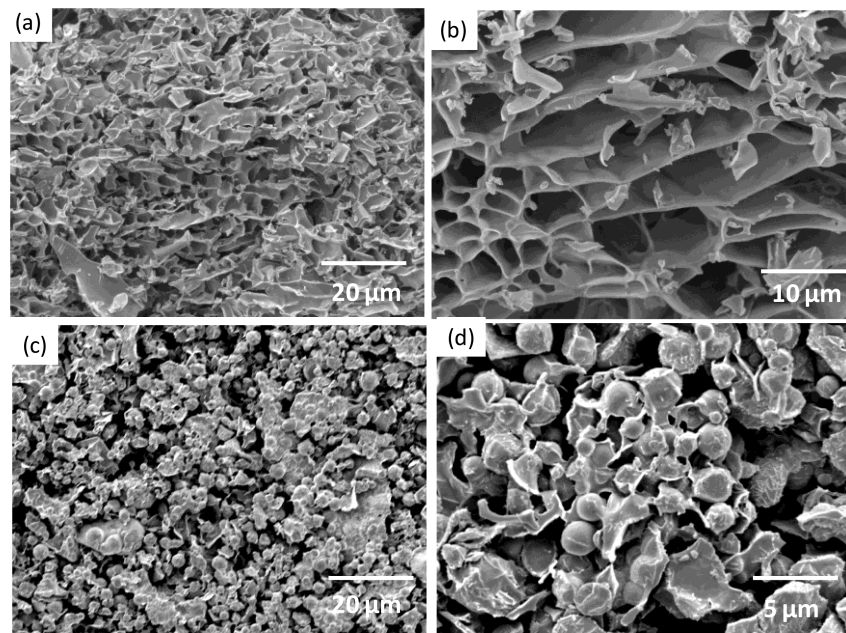


Figure 5. SEM images of freeze-dried (a) PMMA-42AA/3CYS; (b) PMMA-33AA/12DTP; (c) and (d) PMMA-25AA/2CYS gels formed at pH 7.0.

Dynamic Light Scattering (DLS) Analysis. The particle size distributions were investigated by DLS as a function of solution pH, with measurements carried out at pH values ranging from 6.0–10.0. Examples of size distributions for PMMA-27AA non-cross-linked particles are shown in Figure S6a, Supporting Information. The D_h values are summarized in Table S1, Supporting Information. For the dispersions of non-cross-linked PBA-42MAA and PMMA-27AA particles the distributions were monomodal at all pH values tested, while for the PMMA-34AA and PMMA-45AA particle dispersions two or three modes were apparent at pH 10.0. For PMMA-34AA, PMMA-45AA, and PBA-42MAA the variations of the D_h of the dominant particles, D_h^{slow} , with the solution pH are presented in Figure 4a. For all PMMA-AA non-cross-linked particles, increasing the pH resulted in gradual dissociation of any large particles which were present into smaller aggregates, which eventually dissolved completely.

The particle disintegration process is attributed to the ionization of COOH groups along the polymer chains which weaken their associative hydrophobic interactions and increase particle solvation. As the pH increases the polymer chains gradually become hydrophilic enough to overcome the intermolecular forces between adjacent water molecules and fully dissolve. For all PMMA-AA copolymers the initial decrease in D_h at low pH is gradual and is followed by a sharp decrease in particle dimensions at the highest pH, indicating that dissolution of the particles occurs above their respective pK_a values, when ionization is extensive. The particles formed from PMMA-AA with higher acrylic acid content (i.e., those which are more hydrophilic) are larger and less stable to pH induced disintegration. The largest and least soluble particles were observed in the PBA-42MAA particles' dispersions. This could be due to the greater hydrophobicity of PBA compared to PMMA segments.

pH-Triggered swelling, rather than disintegration, was observed in PMMA-AA particles cross-linked with either CYS or DTP at physiological pH values. Compared to the non-cross-linked particles, dispersions of cross-linked particles

showed an initial sharp increase in D_h which was followed by a subsequent decrease at higher pH values (Figure 4b and Figure S7, Supporting Information). Representative cross-linked particle size distributions for PMMA-42AA/3CYS are shown in Figure S6b, Supporting Information. The corresponding D_h values are summarized in Table S1, Supporting Information. For the PMMA-AA particle dispersions the distributions were monomodal at all pH values tested. At pH 6.0, large particles with D_h from 2725 to 4789 nm were observed which increased from 5337 to 5560 nm as the pH was increased to 7.0 (Table S1, Figure S6, Supporting Information). pH-Triggered particle swelling has also been reported in PMMA-MAA and PEA-MAA particles cross-linked with either CYS or DTP,^{31,32,34} where the swelling process was attributed to electrostatic repulsion between negatively charged carboxylate groups in the polymers which are effectively held together by their cross-links.^{56,57} As the pH increases, the disulfide groups, which are present in CYS and DTP, undergo hydroxide ion-mediated cleavage.^{58,59} As a result, the individual polymer chains gradually dissolve as the particles disintegrate and their dimensions are reduced. At pH 10.0, particles with D_h of about 220–3474 nm were observed, indicating that pH-triggered particle dissolution had occurred.⁵⁸ In contrast to their PMMA-AA-derived counterparts, the PBA-41MAA/1DTP particles did not swell in response to increasing pH but instead gradually disintegrated into unimers or small clusters, which is similar to what has been observed in aqueous dispersions of the non-cross-linked PBA-42MAA (Table S1, Supporting Information; compare entries 10 and 11). These results imply that the low degrees of cross-linking for these particles were insufficient for pH-triggered swelling to occur.

The maximum swelling values (Q_{\max}) for all cross-linked particles are presented in Table 2. In each case, Q_{\max} was observed at pH 7.0 which correlates well with the pK_a values of the corresponding (parent) non-cross-linked particles (see Table 1). The Q values for all cross-linked particle dispersions at various pH values are listed in Table S1, Supporting Information. Swelling ratios of up to 3.9 and 8.3 for CYS- and

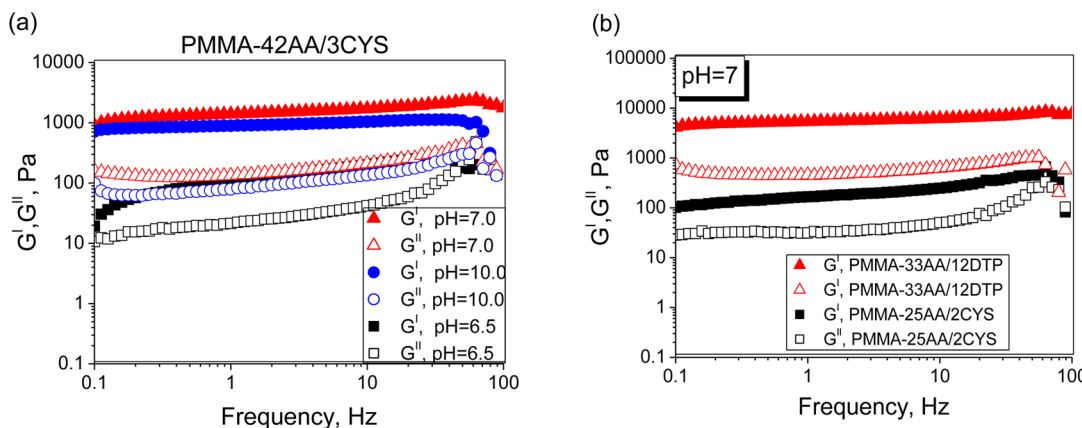


Figure 6. Variation of G' and G'' with the frequency for (a) PMMA-42AA/3CYS at pH 6.5, 7.0 and 10.0; (b) PMMA-33AA/12DTP and PMMA-25AA/2CYS at pH 7.0 (the frequency-sweep data were measured at a strain of 0.1%).

DTP-functionalized particles, respectively, were measured. For both PMMA-AA/CYS and PMMA-AA/DTP the largest Q_{\max} values were observed for the particles featuring the highest AA content (Figure 4c). PMMA-AA/DTP particles have been found to swell to a larger extent than those which are cross-linked with a comparable proportion of CYS. The larger swelling ratios observed for DTP-containing cross-linked particles have been proposed by us to be due to the increased length of the DTP molecule compared to CYS³² and this is supported by the present findings. The effect of the cross-linker structure (CYS versus DTP) upon the mechanical properties of the gels is discussed below.

Compared to the corresponding MAA-containing cross-linked particles,^{31,32,34} Q_{\max} values for the PMMA-AA/CYS and PMMA-AA/DTP particles are lower. This is unexpected in terms of the higher hydrophilicity of AA relative to MAA. For the PMMA-AA-based cross-linked particles it is possible that the original $D_{h(\text{collapse})}$ values are actually relatively high, which would then result in a lower Q_{\max} value; i.e., the “collapsed” state is not fully collapsed.

Gel Morphology. In order to compare the properties of the novel PMMA-AA/CYS and PMMA-AA/DTP particle gels with those of previously studied systems^{31,32,34} a constant particle concentration of 5 wt % has been used for pH-triggered gel formation. The gels formed in the pH range 7.0–7.5, which is highly desirable for future potential application *in vivo*. Gel formation under these conditions is due to the large effective volume fraction occupied by the swollen particles. The particles swell to the point of interparticle contact and this physically locks them into their locations.^{31,32,34} At this point the gels are able to distribute load throughout a network of physically interconnected particles. Representative SEM images of freeze-dried gels formed from swollen PMMA-42AA/3CYS and PMMA-33AA/12DTP particles, at pH 7.0, are shown in Figure 5. The PMMA-42AA/3CYS (Figure 5a), PMMA-33AA/12DTP (Figure 5b), and PMMA-19AA/15DTP gels have highly porous structures. The pore sizes range from 1 to 5 μm and are generally comparable to those observed in their corresponding cross-linked particle precursors (Figure 3). For the PMMA-25AA/2CYS (Figure 5c and d), PMMA-25AA/2DTP, and PMMA-31AA/3CYS gels the majority of cross-linked particles remained intact and the spherical morphology was evident across the gel networks. The shell thickness of the particles was estimated to be about 1.0 to 1.5 μm . As seen from Figure 5d some of the hollow particles appear to have ruptured.

The lowest degree of maximum swelling was calculated for these systems (see Table 2, entries 1, 2, and 3) and is possibly the reason for insufficient particle overlap and hence weaker gels which feature lower elasticity and ductility, as shown by the dynamic rheological data.

Mechanical Properties of the Gels. Dynamic rheology measurements were performed with 5 wt % of the cross-linked PMMA-AA particle dispersions at solution pH values ranging from 6.0 to 10.0. The frequency-sweep studies were carried out at 0.1–100 Hz and at a constant strain of 0.1%. The variation of G' and G'' with the oscillatory frequencies for PMMA-42AA/3CYS, PMMA-31AA/3CYS, PMMA-25AA/2DTP, and PMMA-19AA/15DTP at pH 6.5, 7.0, and 10.0 are shown in Figure 6a and in Figure S8, Supporting Information. For all systems studied, very low moduli values were observed at the lower pH values. As the pH increases the elastic modulus values increase. Gels with optimum elasticity values were observed at physiological pH values. At low frequency and at all pH values tested, all systems behaved as elastic gels with a storage modulus, G' , larger than the loss modulus, G'' . As the frequencies increased, from 40 to 100 Hz, the two moduli tended to diverge, giving rise to flow zones at pH 6.5 and 10.0. At pH 7.0, elastic behavior was observed over the entire frequency range for PMMA-42AA/3CYS (Figure 6a), PMMA-19AA/15DTP (Figure S8a, Supporting Information), and PMMA-33AA/12DTP (Figure 6b). The data are characterized by G' exhibiting a plateau which is indicative of a stable cross-linked network. Figure 6b gives the frequency sweep data for PMMA-25AA/2CYS and PMMA-33AA/12DTP at pH 7.0 which typify the rheological properties of a weak and a strong gel, respectively. Compared to PMMA-33AA/12DTP, the PMMA-25AA/2CYS gel showed a network breakdown at high frequency (from 60 to 100 Hz). Another notable feature is the magnitudes of the moduli, which for PMMA-33A/12DTP were considerably greater than those of PMMA-25AA/2CYS. The gels formed from PMMA-25AA/2DTP (Figure S8b, Supporting Information) and PMMA-31AA/3CYS (Figure S8c, Supporting Information) cross-linked particles were also weak. For the PMMA-25AA/2CYS (Figure 6b) and PMMA-25AA/2DTP (Figure S8b, Supporting Information) physical gels the frequencies at which $G' = G''$ (a critical frequency, f_{crit}) occurred were approximately 79 and 63 Hz, respectively. This corresponds to a critical relaxation time ($\tau_{\text{crit}} = 1/f_{\text{crit}}$) of 0.013 s for PMMA-25AA/2CYS and 0.016 s for rearrangements of PMMA-25AA/2DTP. The shorter relaxation time for PMMA-

25AA/2CYS corresponds to an increased rate at which the interparticle network is repaired under dynamic strain and is consistent with the greater mobility of the PMMA-AA/CYS chains.^{34,60} The data are consistent with our hypothesis that DTP cross-linked gels are able to confer a less flexible conformation compared to CYS.

For the various PMMA-AA/CYS and PMMA-AA/DTP gels the variation of G' and G'' as a function of AA content (mol %) is shown in Figure 7. The data are taken at pH 7.0 with a

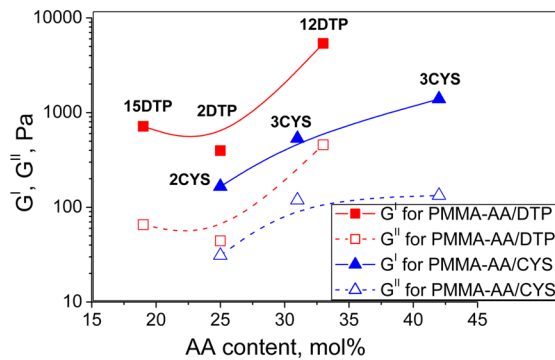


Figure 7. G' and G'' as a function of AA content (mol %) for PMMA-AA/CYS and PMMA-AA/DTP gels at pH 7.0 and frequency of 1 Hz.

frequency of 1 Hz. At lower AA contents, the samples typically have low moduli values which increase as the AA content increases. For both PMMA-AA/CYS and PMMA-AA/DTP the largest moduli values were observed for the gels featuring the

highest AA content. For these gels the highest swelling ratio of the corresponding cross-linked particle precursors was also observed (see Table 2). A possible explanation is that the higher AA content results in an increased extent of interparticle contact and hence the number density of elastically effective chains is also greater. Compared to PMMA-AA/CYS, the PMMA-AA/DTP gels are stronger with elastic moduli values up to four times greater than those of the CYS-functionalized gels. This has been previously rationalized by considering the different conformational constraints and rigidities of the CYS and DTP cross-link units.^{32,61} The DTP-cross-linked gels possess less freedom of movement compared to the CYS-functionalized structures and are therefore able to confer a more rigid, extended conformation upon the elastically effective chains. The lowest moduli values were observed for the sparsely cross-linked PMMA-25AA/2CYS, PMMA-25AA/2DTP, and PMMA-31AA/3CYS gels, which feature lower AA content. For these gels, rupturing of the intact spherical hollow particles was evidenced from the SEM images (see Figure 5c,d).

Strain-sweep dynamic rheology experiments were performed on the cross-linked particle gels over a broad pH range (from pH 6.0 to pH 10.0) and at a constant frequency of 1 Hz. The strain sweep data for PMMA-42AA/3CYS at pH 6.5, 7.0, and 10.0 are shown in Figure 8a. For the remaining PMMA-AA/CYS and PMMA-AA/DTP gels the data are presented in Figure S9, Supporting Information. At low strain (γ), less than 10% all dispersions show elastic responses, with $G' > G''$, whereas at higher deformations the response was clearly nonelastic. The critical yield strain (γ_c) is the γ value

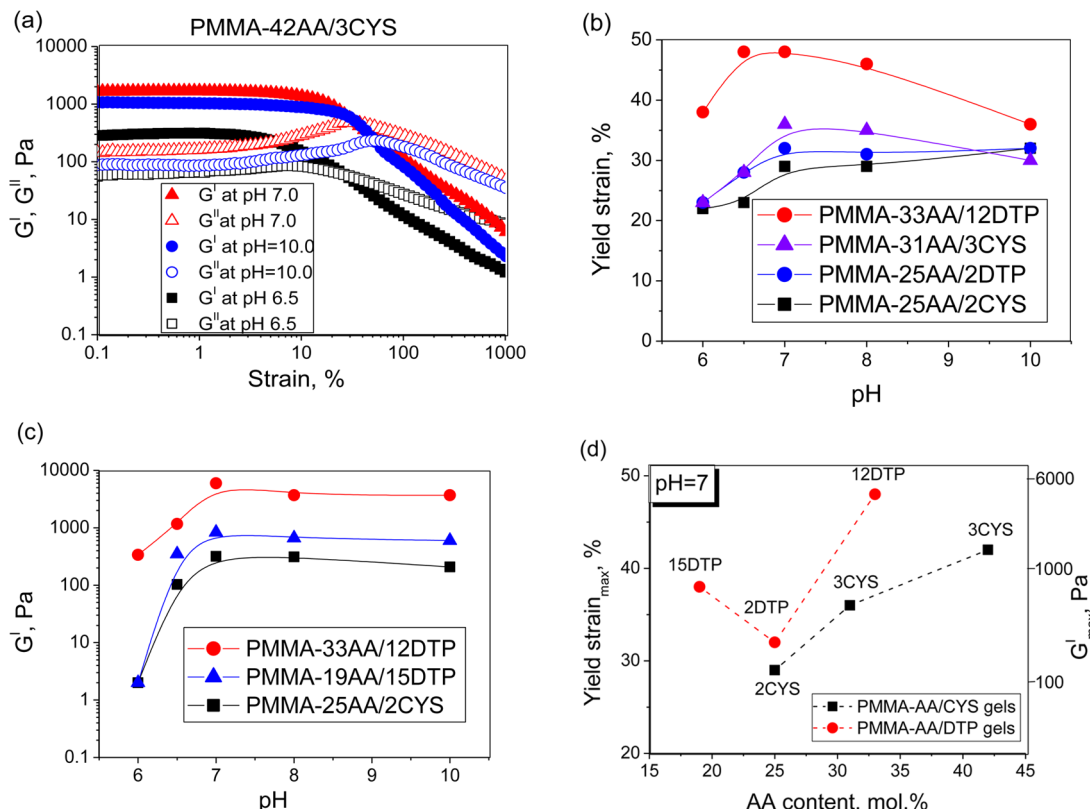


Figure 8. (a) G' and G'' as a function of strain percentage for PMMA-42AA/3CYS at pH 6.5, 7.0, and 10.0; (b) yield strain as a function of the solution pH for PMMA-AA/CYS and PMMA-AA/DTP particle concentrated dispersions; (c) variation of G' with pH for PMMA-AA/CYS and PMMA-AA/DTP; the data were measured at a strain of 1%; (d) variation of $\gamma_c(\text{max})$ and G'_{max} with AA content (mol %) for PMMA-AA/CYS and PMMA-AA/DTP gels; the data were recorded at pH 7.0, a frequency of 1 Hz, and strain of 1%.

corresponding to a crossover point where $G' = G''$. When γ is greater than γ_c the gel is considered to be fluid and most of the energy is lost as heat. The variations of γ_c with the solution pH for selected PMMA-AA/CYS and PMMA-AA/DTP concentrated dispersions are shown in Figure 8b. The initial increase in pH results in an increase in γ_c up to pH 7.0, followed by a decrease. For each gel the maximum γ_c ($\gamma_{c(\max)}$) value was recorded at pH 7.0; the maximum values of G' (G'_{\max}) and G'' (G''_{\max}) for the gels were also observed at this pH (Figure 8c and Figure S10, Supporting Information). Values for the G'_{\max} of each gel and the corresponding pH ($pH_{G'_{\max}}$) and $\gamma_{c(\max)}$ are shown in Table 2. Interestingly, the $pH_{G'_{\max}}$ values correspond to the pH where Q_{\max} occurs, demonstrating a strong correlation between maximum particle swelling, gel elasticity, and gel ductility. The variation of G'_{\max} and $\gamma_{c(\max)}$ with AA content for all PMMA-AA-based gels are presented in Figure 8d. An unexpected result in this study was that both G' and yield strain increase linearly with AA content. For the PMMA-AA/CYS gels the G'_{\max} and $\gamma_{c(\max)}$ values were found to decrease in the following order: PMMA-42AA/3CYS > PMMA-31AA/3CYS > PMMA-25AA/2CYS. For the PMMA-AA/DTP gels the decrease follows the order: PMMA-33AA/12DTP > PMMA-19AA/15DTP > PMMA-25AA/2DTP. The corresponding AA contents and swelling ratios also decrease in the same orders (see Table 2). The decrease in moduli magnitudes and gel ductilities with decreasing AA content can be rationalized by the decreasing level of interparticle contact, which is an integral part of gel formation. The lightly cross-linked PMMA-25AA/2CYS and PMMA-25AA/2DTP gels exhibited the lowest ductilities presumably because they are too weak to respond reversibly to applied deformation stresses. The SEM images of these gels show intact spherical cross-linked particles across the gels' networks (see Figure 5c,d). The most elastic gels, derived from PMMA-42AA/3CYS and PMMA-33AA/12DTP, were able to deform rapidly and reversibly in response to the strain (Figure 5a,b). For these gels the SEM images show highly porous and interconnected structures. Compared to PMMA-AA/DTP the corresponding CYS-functionalized gels are considerably less elastic and ductile. The results are closely related to the frequency sweep data where the DTP-functionalized gels demonstrated higher network stability and smaller τ_{crit} values.

Biodegradability of pH-Responsive PMMA-AA/CYS and PMMA-AA/DTP Gels. The potential biodegradability of the new AA-containing cross-linked particle gels was tested using glutathione, a naturally occurring reducing agent which is present throughout the human body. The addition of a 5 mM solution of glutathione (intracellular concentration) to each of the gels immediately resulted in large decreases in the gels' elasticities. The gel-to-fluid transitions of the PMMA-31AA/3CYS and PMMA-33AA/12DTP networks following the addition of glutathione are shown in Figure 9 and Figure S11, Supporting Information. For the PMMA-31AA/3CYS gel, the addition of glutathione resulted in network breakdown after 15 min. After this time the gel began to flow and its viscous properties were dominant ($G' < G''$). The rate of network disassembly was found to be strongly dependent upon the gel's structure. For the PMMA-AA/DTP gels the time for gel-to-fluid transition was considerably larger than that for the PMMA-AA/CYS gels (compare Figure 9 with Figure S11, Supporting Information). This finding demonstrates the importance of the gel's structure on its properties and performance.

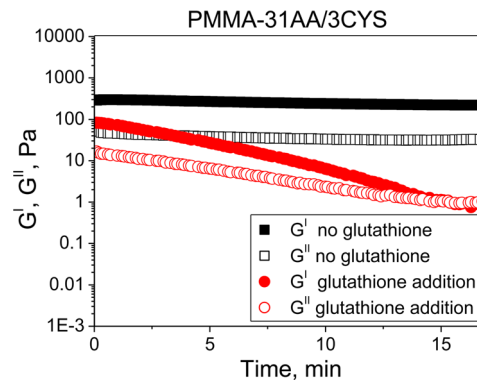


Figure 9. Biodegradability of PMMA-31AA/3CYS, determined by addition of glutathione solution (data were obtained at pH 7.0).

Biocompatibility Studies of PMMA-AA/CYS and PMMA-AA/DTP Gels. MTT cell viability assays were used to measure the response of immortalised human chondrocyte cells to the addition of PMMA-33AA/12DTP gel samples with total weights of 5, 10, 15, 20, and 25 mg. The results indicated the absence of any significant cell disruption at the various gel doses for 24 h (see Figure S12a, Supporting Information). The MTT cell viability assays for the remaining gels were performed by addition of 20 mg gel into the well inserts for 8, 24, and 48 h. The wells were seeded with 6×10^4 immortalized human chondrocyte cells with a total cell culture volume of 1 mL. The cell media was in direct contact with the gels, which were used as received and not purified additionally before use. For all gels the data showed a reduction in cell activity with time compared to the control using cells alone (Figure 10a and b). The percentage cell viability decreased to 71.4% for PMMA-42AA/3CYS and 67.0% for PMMA-19AA/15DTP, indicating a significant level of cytotoxicity for these gels.⁶² However, the cell viability for the PMMA-19AA/15DTP appears to have stabilized at 48 h. Representative light microscopy and Live/Dead assay phase-contrast images of cells taken after 48 h incubation with PMMA-33AA/12DTP gel are shown in Figure 10d and f. The data are compared to control images (Figure 10c,e) which show cell regions that were not in contact with the gels. The optical microscope and Live/Dead assay images for PMMA-31AA/3CYS are presented in Figure S12c and S12e, Supporting Information. The data in Figures 10d and S12c show that the cells preserved their elongated morphology and were still attached. There was no evidence of cell death as seen by the green (live) fluorescent images in Figures 10f and S12e (Supporting Information). The cytotoxicity results revealed that our new PMMA-31AA/CYS, PMMA-25AA/2CYS, PMMA-25AA/2DTP, and PMMA-33AA/12DTP gels show very good biocompatibility, with at least 80% cell viability after 48 h. For the PMMA-AA/DTP and PMMA-AA/CYS gels, increases in the cross-linking density and AA content, respectively, appear to decrease the cell viability. An advantage of these systems for potential application in tissue engineering is that PMMA is used in bone cement. Furthermore, MMA-containing biomaterials have shown various benefits in clinical applications.⁶³

Impact of the Polymer Structure on Gel Properties and Cytotoxicity. Our studies clearly show that small chemical modifications in the polymer structure of poly((meth)acrylic acid)-containing gels can result in large differences in both properties and performance. Although the

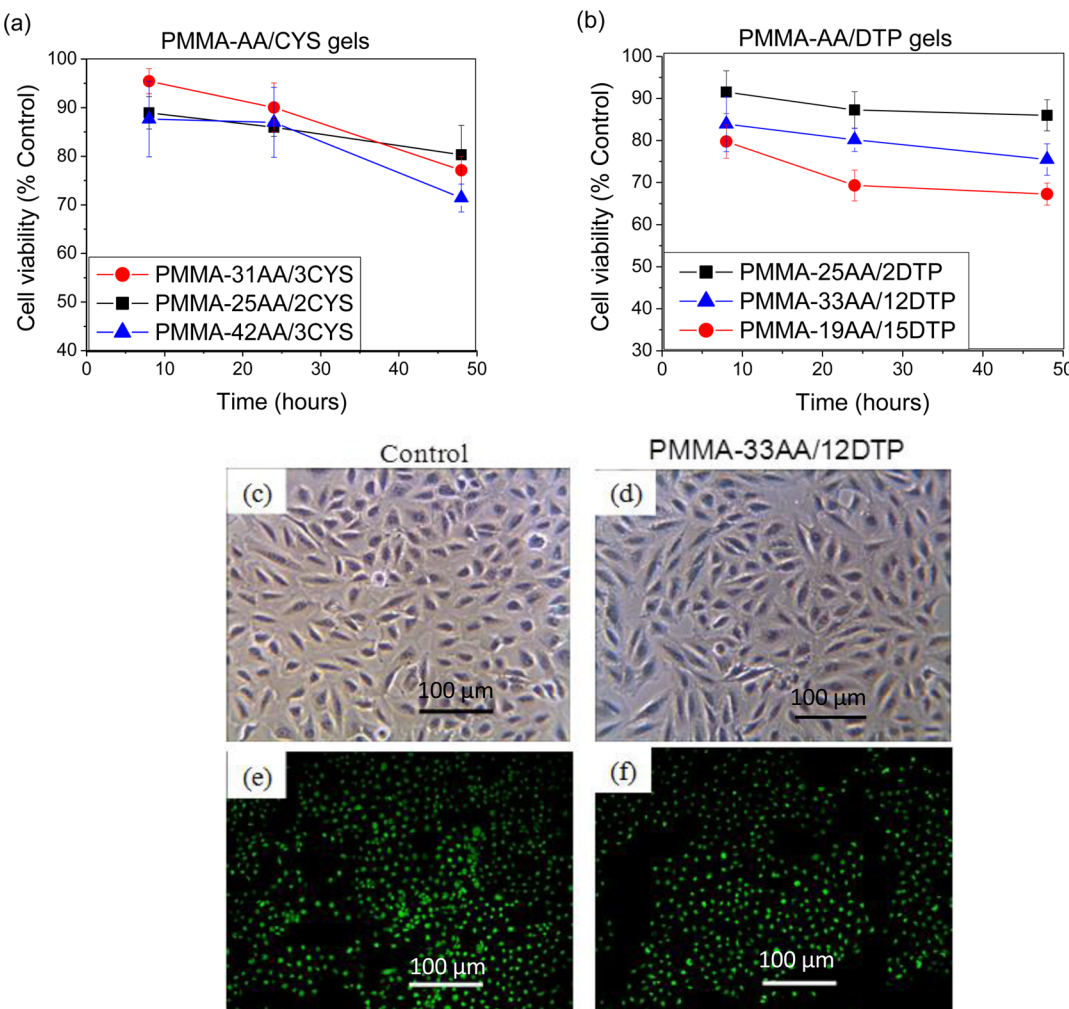


Figure 10. Cytotoxicity assessment for PMMA-AA/CYS and PMMA-AA/DTP gels, MTT assay for 20 mg: (a) PMMA-AA/CYS and (b) PMMA-AA/DTP, gels immersed in culture media in contact with human chondrocyte cells for 8, 24, and 48 h. (c) Optical micrographs of cells that were not in contact with the gel (control); (d) chondrocyte cells in contact with PMMA-33AA/12DTP gel; (e) Live/Dead assay of chondrocyte cells that were not in contact with the gel (control); (f) Live/Dead assay of chondrocyte cells in contact with PMMA-33AA/12DTP gel. All images were taken after 48 h.

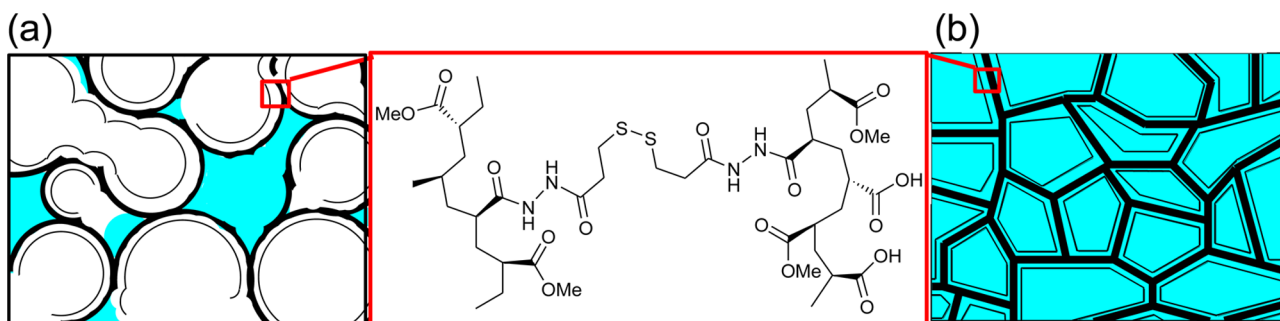


Figure 11. Representation of PMMA-AA/DTP particle gels with low (a) and high (b) elasticity.

fundamental mechanism for gel formation and the linear relationship between the value of G' and a hydrogel's swelling ratio were not altered upon substitution of the MAA units for AA, the PMMA-AA-based gels' strengths and ductilities were all considerably lower than those of the analogous PMMA-MAA/CYS and PMMA-MAA/DTP cross-linked particle gels.³² For the MAA- and AA-based gels the process of gelation involves interpenetration of the shells of the swollen cross-linked particles at a sufficiently high concentration and appropriate

solution pH value. MAA is more hydrophobic than AA; therefore, PMMA-AA cross-linked particle gels (Figure 11) would be expected to absorb more water than their PMMA-MAA analogues.⁶⁴ For the PMMA-AA gels, elasticity originates from two primary sources: the elastically effective chains within each shell which distribute the strain and the transfer of stress from one hollow particle to the next by intershell contact. A sufficient level of swelling is necessary in order for particle interpenetration and gelation to occur. Indeed, a lower AA

content is associated with both a lower swelling ratio and lower gel mechanical strength within the series of PMMA-AA cross-linked particles studied (see Figure 11a). The increasing Q value (through increasing AA content) will decrease the number density of elastically effective chains and this will decrease the intraparticle elasticity. However, increased intershell contact will occur and this will increase G' for the whole gel, since more elastically effective chains (overall) contribute to the stress distribution across the gel (see Figure 11b). Table 2 shows that the systems with the highest cross-linker concentration (12 mol % and 15 mol % DTP) had the highest G' values and it seems that intraparticle elasticity is important for these systems (Figure 11b). However, their G' values are low compared to the related PMMA-MAA-based systems,³² which could be accounted for by less efficient intershell contact due to the increased hydrophilicity of the AA-containing shells. The sparsely grafted PMMA-MAA-containing systems have a more hydrophobic shell, which is anticipated to enhance intershell contact and the elasticity of the entire gel. Compared to the hydrogels derived from natural polymers such as collagen, chitosan, alginate, agarose, and silk, the elasticity and ductility of PMMA-AA hollow particle gels are considerably lower.⁶⁵ However, the PMMA-AA particle gels are not intended to be used for load bearing applications. Agarose, alginate, and collagen have been reported to support the regeneration of cartilage in a rabbit model, whereas silk-fiber composite was used for bone repair.⁶⁶

For both PMMA-MAA and PMMA-AA, swelling was observed only in the dispersions of particles which were cross-linked with either DTP or CYS at a pH range from 6.5 to 8.0 (see DLS results, Table S1, Supporting Information). The ability of the particles to swell depends on the extent of the cross-linking and the copolymer's structure as well as pH. For MMA- and AA-containing particle gels the Q_{\max} , G'_{\max} , γ_{\max} and maximum stability were all observed at pH 7.0–7.5, which is an ideal pH range for biological applications. The values of G'_{\max} and γ_{\max} were found to decrease as the molar concentration of the COOH groups decreased (see Figure 8d). These declines in gel elasticity and ductility are attributed to lower levels of interparticle contact, which is an integral part of gel formation. The gels derived from PMMA-AA and PMMA-MAA particles cross-linked with DTP feature considerably higher mechanical strength and ductility than their CYS-functionalized counterparts (see Table 2), suggesting that the extra amide bonds within the DTP molecule impart an increased degree of rigidity to the interchain linkages. The DTP-functionalized gels also exhibit improved interconnectivity (see Figure 5). The new physical gels derived from the MMA-containing cross-linked particles demonstrated excellent biodegradability. The rate of network biodegradability was found to be lower for the stronger and more ductile gels. For the PMMA-31AA/3CYS gels less than 16 min was required for the gel to become liquid, compared to approximately 26 min for PMMA-33AA/12DTP (Figures 9 and S11, Supporting Information). Gel composition has also been found to affect biocompatibility. For the PMMA-AA/DTP gels, a higher cross-link density correlated with reduced cell viability, whereas an increase in the percentage AA content of the PMMA-AA/CYS gels decreased the level of cell viability.

The potential for PBA-MAA and PMA-MAA to form gels under physiological pH conditions was also studied. However, due to the higher hydrophobicity of PBA (compared to PMA and PMMA) the pK_a values for the PBA-42MAA particles were

also much higher. Furthermore, as PBA contains the sterically cumbersome *n*-butyl groups, it is possible that some of the COOH groups are buried within the hydrophobic PBA interior and therefore not available for cross-linking. In fact, the lowest percentage of amide formation was observed for PBA-41MAA/1DTP. Furthermore, no cross-linking was observed from the reaction of PBA-42MAA with CYS. The PBA-41MAA/1DTP does not form gels at all, which has been attributed to the strongly hydrophobic nature of the copolymer. The PMA-40MAA particles did not redisperse after centrifugation which was attributed to the greater flexibility of PMA relative to the PMMA. The present study clearly shows that appropriate copolymer design is an essential criterion for physical gelation to occur.

CONCLUSIONS

In the present study we have synthesized and investigated the properties of PMMA-AA, PBA-MAA, and PMA-MAA copolymers in order to increase our overall understanding of these types of materials and optimize the copolymer design for the preparation of new pH-sensitive gel scaffolds for non-load-bearing tissue repair. Physical gels were formed in the physiological pH range only from concentrated dispersions of hollow PMMA-AA particles, which were cross-linked with either CYS or DTP. The PMA-40MAA particles did not redisperse after centrifugation, whereas for the PBA-MAA particles only a 3% yield of DTP incorporation was achieved, which was found to be insufficient for physical gelation to occur. The study confirms that MMA is the optimal ester and DTP is a superior cross-linker to CYS for the formation of elastic, biodegradable, and biocompatible carboxylic acid-containing physical gels. Furthermore, it has been suggested that the pH-triggered swelling transition near physiological pH will occur not only upon substitution of MAA for AA but also when a range of various carboxylic acid-containing monomers are utilized.

The pH-dependent swelling and disassembly of the hollow PMMA-AA particles before and after cross-linking were studied using DLS. The particles' Q_{\max} values showed a linear relationship with the gels' G'_{\max} and γ_{\max} values. Networks formed from the PMMA-AA/CYS and PMMA-AA/DTP gels featuring the highest AA content were the strongest, most ductile, and most stable. Furthermore, compared to PMMA-AA/CYS the corresponding DTP-functionalized gels were considerably more elastic and ductile, with the PMMA-33AA/12DTP gel featuring the most optimal properties. For this gel a significant improvement in porosity and physical characteristics (i.e., moduli and ductility) was achieved. Compared to the previously reported PMMA-MAA/CYS and PMMA-MAA/DTP gels, the PMMA-AA-derived gels described herein were composed of hydrophilic, well-presented, hollow particles with increased intraparticle elasticity. A hypothetical model was developed in order to explain the physical gelation in PMMA-AA particle gels (Figure 11). PMMA-AA gels show good biodegradability and biocompatibility. The biodegradability and cytotoxicity were tuneable through particle composition. Because the new PMMA-AA gels are biodegradable and biocompatible, featuring high interconnected porosity and adequate mechanical strength, they are a promising prototype for injectable gels for nonload tissue repair and also drug delivery applications.

ASSOCIATED CONTENT

Supporting Information

GPC traces for PMMA-AA, PBA-42AA, and PMA-40AA copolymers, ^1H NMR spectra of PMMA-27AA and PBA-42AA copolymers, SEM images of PBA-42MAA non-cross-linked particles, potentiometric titration data for non-cross-linked PMMA-AA and PBA-42AA particles, variation of the hydrodynamic diameter (D_h) with pH for non-cross-linked and cross-linked particles, size distribution functions for non-cross-linked and cross-linked PMMA-AA particles taken at different pH values, particle size as a function of pH for selected PMMA-AA cross-linked particles, frequency, and strain sweep data for selected PMMA-AA cross-linked particle gels studied, biodegradability, and biocompatibility results for representative PMMA-AA cross-linked particle gels. This material is available free of charge via the Internet at <http://pubs.acs.org>.

AUTHOR INFORMATION

Corresponding Authors

*E-mail: S.Halacheva@bolton.ac.uk; Tel: +44 (0)1204 903725.
*E-mail: Brian.Saunders@manchester.ac.uk; Tel: +44 (0)161 306 5944.

Notes

The authors declare no competing financial interest.

ACKNOWLEDGMENTS

The authors would like to thank the EPSRC for funding this study.

REFERENCES

- (1) Drury, J. L.; Mooney, D. J. *Biomaterials* **2003**, *24*, 4337–4351.
- (2) Kouwer, P. H. J.; Koepf, M.; Le Sage, V. A. A.; Jaspers, M.; van Buul, A. M.; Eksteen-Akeroyd, Z. H.; Woltinge, T.; Schwartz, E.; Kitto, H. J.; Hoogenboom, R.; Picken, S. J.; Nolte, R. J. M.; Mendes, E.; Rowan, A. E. *Nature* **2013**, *493*, 651–655.
- (3) Van Vlierberghe, S.; Dubruel, P.; Schacht, E. *Biomacromolecules* **2011**, *12*, 1387–1408.
- (4) Tan, H.; Chu, C. R.; Payne, K. A.; Marra, K. G. *Biomaterials* **2009**, *30*, 2499–2506.
- (5) Vashist, A.; Shahabuddin, S.; Gupta, Y. K.; Ahmad, S. *J. Mater. Chem. B* **2013**, *1*, 168–178.
- (6) Benoit, D. S.; Schwartz, M. P.; Durney, A. R.; Anseth, K. S. *Nat. Mater.* **2008**, *7*, 816–823.
- (7) Hoare, T. R.; Kohane, D. S. *Polymer* **2008**, *49*, 1993–2007.
- (8) Hoffman, A. S. *J. Controlled Release* **1987**, *6*, 297–305.
- (9) Kloxin, A. M.; Kasko, A. M.; Salinas, C. N.; Anseth, K. S. *Science* **2009**, *324*, 59–63.
- (10) Lee, K. Y.; Mooney, D. J. *Chem. Rev.* **2001**, *101*, 1869–1880.
- (11) Oh, J. K.; Tang, C.; Gao, H.; Tsarevsky, N. V.; Matyjaszewski, K. *J. Am. Chem. Soc.* **2006**, *128*, 5578–5584.
- (12) Hoffman, A. S. *Adv. Drug Delivery Rev.* **2002**, *43*, 3–12.
- (13) Tai, H.; Howard, D.; Takae, S.; Wang, W.; Vermonden, T.; Hennink, W. E.; Stayton, P. S.; Hoffman, A. S.; Endruweit, A.; Alexander, C.; Howdle, S. M.; Shakesheff, K. M. *Biomacromolecules* **2009**, *10*, 2895–2903.
- (14) Thornton, P. D.; Billah, S. M. R.; Cameron, N. R. *Macromol. Rapid Commun.* **2013**, *34*, 257–262.
- (15) Halacheva, S.; Rangelov, S.; Tsvetanov, Ch. *J. Phys. Chem. B* **2008**, *112*, 1899–1905.
- (16) Halacheva, S.; Rangelov, S.; Tsvetanov, Ch.; Garamus, V. M. *Macromolecules* **2010**, *43*, 772–781.
- (17) Li, Y.; Armes, S. P. *Macromolecules* **2005**, *38*, 8155–8162.
- (18) Oh, J. K.; Siegwart, D. J.; Lee, H.; Sherwood, J.; Peteanu, L.; Hollinger, J. O.; Kataoka, K.; Matyjaszewski, K. *J. Am. Chem. Soc.* **2007**, *129*, 5939–5945.
- (19) Tsarevski, N. V.; Matyjaszewski, K. *Macromolecules* **2005**, *38*, 3087–3092.
- (20) Sun, K. H.; Sohn, Y. S.; Jeong, B. *Biomacromolecules* **2006**, *7*, 2871–2877.
- (21) Schu, X. Z.; Liu, Y.; Luo, Y.; Roberts, M. C.; Prestwich, G. D. *Biomacromolecules* **2002**, *3*, 1304–1311.
- (22) Ghosh, K.; Shu, X. Z.; Mou, R.; Lombardi, J.; Prestwich, G. D.; Rafailovich, M. H.; Clark, R. A. F. *Biomacromolecules* **2005**, *6*, 2857–2865.
- (23) Lee, Y.; Chung, H. J.; Yeo, S.; Ahn, C. H.; Lee, H.; Messersmith, P. B.; Park, T. G. *Soft Matter* **2010**, *6*, 977–983.
- (24) Hutmacher, D. W. *Biomaterials* **2000**, *21*, 2529–2543.
- (25) Richardson, S. M.; Curran, J. M.; Chen, R.; Vaughan-Thomas, A.; Hunt, J. A.; Freemont, A. J.; Hoyland, J. A. *Biomaterials* **2006**, *27*, 4069–4078.
- (26) Elisseeff, J. H.; Lum, L. *Injectable Hydrogels for Cartilage Tissue Engineering*. In *Topics in Tissue Engineering, Volume 1*; Ashammakhi N., Ferretti P., Eds.; 2003 (accessed from http://www.oulu.fi/spareparts/ebook_topics_in_t_e/cover.html, January 2014).
- (27) Lee, K. Y.; Alsberg, E.; Mooney, D. J. *J. Biomed. Mater. Res.* **2001**, *56*, 228–233.
- (28) Lisignoli, G.; Fini, M.; Giavaresi, G.; Nicoli Aldini, N.; Toneguzzi, S.; Facchini, A. *Biomaterials* **2002**, *23*, 1043–1051.
- (29) Kundu, B.; Kundu, S. C. *Biomaterials* **2012**, *33*, 7456–7467.
- (30) Liu, X.; Jin, X.; Ma, P. X. *Nat. Mater.* **2011**, *10*, 398–406.
- (31) Bird, R.; Freemont, T.; Saunders, B. R. *Soft Matter* **2012**, *8*, 1047–1057.
- (32) Halacheva, S. S.; Freemont, T. J.; Saunders, B. R. *J. Mater. Chem. B* **2013**, *1*, 4065–4078.
- (33) Vercruyse, K. P.; Marecak, D. M.; Marecek, J. F.; Prestwich, G. D. *Bioconjugate Chem.* **1997**, *8*, 686–694.
- (34) Bird, R.; Freemont, T.; Saunders, B. R. *Chem. Commun.* **2011**, *47*, 1443–1445.
- (35) Chen, Y.; Ding, D.; Mao, Z.; He, Y.; Hu, Y.; Wu, W.; Jiang, X. *Biomacromolecules* **2008**, *9*, 2609–2614.
- (36) Zhu, Y.; Meng, W.; Gao, H.; Hanagata, N. *J. Phys. Chem. C* **2011**, *115*, 13630–13636.
- (37) Patton, J. N.; Palmer, A. F. *Biomacromolecules* **2005**, *6*, 414–424.
- (38) Fan, J.-B.; Huang, C.; Jiang, L.; Wang, S. *J. Mater. Chem. B* **2013**, *1*, 2222–2235.
- (39) Champon, P.; Blanazs, A.; Battaglia, G.; Armes, S. P. *Macromolecules* **2012**, *45*, 5081–5090.
- (40) Li, Y.; Peng, B.; Chen, Y. *J. Mater. Chem. B* **2013**, *1*, 5694–5701.
- (41) Lee, J.-H.; Gustin, J. P.; Chen, T.; Payne, G. F.; Raghavan, S. R. *Langmuir* **2005**, *21*, 26–33.
- (42) Yao, J.; Feng, Y.; Zhao, Y.; Li, Z.; Huang, J.; Fu, H. *J. Colloid Interface Sci.* **2007**, *314*, 523–530.
- (43) Chen, T.; Du, B.; Fan, Z. *Langmuir* **2012**, *28*, 11225–11231.
- (44) CRC Handbook of Chemistry and Physics, 87th ed.; Lide D. R., Ed.; Taylor & Francis: Boca Raton, 2006.
- (45) Rager, T.; Meyer, W. H.; Wegner, G.; Mathauer, K.; Mächtle, W.; Schrof, W.; Urban, D. *Macromol. Chem. Phys.* **1999**, *200*, 1681–1691.
- (46) Ravi, P.; Wang, C.; Tam, K. C.; Gan, L. H. *Macromolecules* **2002**, *36*, 173–179.
- (47) Echeverria, C.; Peppas, N. A.; Mijangos, C. *Soft Matter* **2012**, *8*, 337–346.
- (48) Saito, R.; Yamaguchi, K.; Hara, T.; Saegusa, C. *Macromolecules* **2007**, *40*, 4621–4625.
- (49) Kuo, J. W.; Swann, D. A.; Prestwich, G. D. *Bioconjugate Chem.* **1991**, *2*, 232–241.
- (50) Nakajima, N.; Ikada, Y. *Bioconjugate Chem.* **1995**, *6*, 123–130.
- (51) Pouyani, T.; Prestwich, G. D. *Bioconjugate Chem.* **1994**, *5*, 339–347.
- (52) Pouyani, T.; Kuo, J. W.; Harbison, G. S.; Prestwich, G. D. *J. Am. Chem. Soc.* **1992**, *114*, 5972–5976.
- (53) Shu, X. Z.; Liu, Y.; Luo, Y.; Roberts, M. C.; Prestwich, G. D. *Biomacromolecules* **2002**, *3*, 1304–1311.

- (54) Hwangbo, K.-H.; Kim, M. R.; Lee, C.-S.; Cho, K. Y. *Soft Matter* **2011**, *7*, 10874–10878.
- (55) Krzyzanek, V.; Sporenberg, N.; Keller, U.; Guddorf, J.; Reichelta, R.; Schönhoff, M. *Soft Matter* **2011**, *7*, 7034–7041.
- (56) Kokufuta, E.; Wang, B.; Yoshida, R.; Khokhlov, A. R.; Hirata, M. *Macromolecules* **1998**, *31*, 6878–6884.
- (57) Philippova, O. E.; Hourdet, D.; Audebert, R.; Khokhlov, A. R. *Macromolecules* **1997**, *30*, 8278–8285.
- (58) Thakur, S. S.; Balaram, P. *J. Am. Soc. Mass Spectrom.* **2009**, *20*, 783–791.
- (59) Galande, A. K.; Trent, J. O.; Spatola, A. F. *Biopolymers* **2003**, *71*, 534–551.
- (60) *Polymer Handbook*, 4th ed.; Brandrup J., Immergut E. H., Grulke E. A., Abe A., Block D. R., Eds.; Wiley: New York, 1999.
- (61) Gilbert, H. F. Peptide Bonds, Disulfide Bonds and Properties of Small Peptides. In *Encyclopedia of Life Sciences (ELS)*; John Wiley & Sons, Ltd: Chichester, 2010.
- (62) Patenaude, M.; Campbell, S.; Kinlo, D.; Hoare, T. *Biomacromolecules* **2014**, *15*, 781–790.
- (63) Seal, B. L.; Otero, T. C.; Panitch, A. *Mater. Sci. Eng., R: Rep.* **2001**, *34*, 147–230.
- (64) Ratner, B. In *Biomaterials Science: An Introduction to Materials in Medicine*, 3rd ed.; Elsevier: Oxford, 2013.
- (65) Willerth, S. M.; Sakiyama-Elbert, S. E. Combining Stem Cells and Biomaterial Scaffolds for Constructing Tissues and Cell Delivery; Bhatia S., Polak J., Eds.; *The Stem Cell Research Community, StemBook*; DOI 10.3824/stembook.1.1.1; <http://www.stembook.org>.
- (66) Mandal, B. B.; Grinberg, A.; Gil, E. S.; Panilaitis, B.; Kaplan, D. L. *Proc. Natl. Acad. Sci. U.S.A.* **2012**, *109*, 7699–7704.

■ NOTE ADDED AFTER ASAP PUBLICATION

This paper was published ASAP on April 14, 2014, with the name of author Eseelle K. Hendow omitted. The corrected version was reposted on May 1, 2014.